ELSEVIER

Journal of Electron Spectroscopy and Related Phenomena 126 (2002) 67–76

JOURNAL OF ELECTRON SPECTROSCOPY and Related Phenomena

www.elsevier.com/locate/elspec

Development of the scattering theory of X-ray absorption and core level photoemission

J.J. Rehr[a], W. Schattke[b], F.J. García de Abajo[c], R. Díez Muiño[d], M.A. Van Hove[e,f,*]

[a] *Department of Physics, University of Washington, Seattle, WA 98195-1560, USA*
[b] *Institut für Theoretische Physik und Astrophysik, Christian-Albrechts-Universität zu Kiel, D-24098 Kiel, Germany*
[c] *Centro Mixto CSIC-UPV/EHU, ES-20080 San Sebastián, Spain*
[d] *Donostia International Physics Center (DIPC), ES-20018 San Sebastián, Spain*
[e] *Materials Sciences Division and Advanced Light Source, Lawrence Berkeley National Laboratory, Berkeley, CA 94720, USA*
[f] *Department of Physics, University of California at Davis, Davis, CA 95616, USA*

Abstract

Over the past two decades dramatic progress has been made in the development of the theory of X-ray and electron spectroscopies, e.g., X-ray absorption spectra (XAS), core-level X-ray photoemission spectroscopy (XPS), X-ray photoelectron diffraction (XPD), etc. A revolutionary advance was the development of efficient and accurate treatments of high-order, curved-wave electron multiple-scattering for high electron energies above a few hundred eV. These advances were applied first in the theory of X-ray absorption fine structure (XAFS) and subsequently in X-ray photoelectron diffraction (XPD). They also led to efficient ab initio codes which permit a quantitative interpretation of the spectra. Extensions have made it possible to treat magnetic effects, e.g., X-ray magnetic circular dichroism (XMCD) and its analog in XPD. Important progress has recently been made in understanding near-edge spectra, e.g. X-ray absorption near edge spectra (XANES), which often require a full-multiple-scattering treatment. Although such calculations had been highly demanding computationally, fast new approaches based on efficient Lanczos approaches and parallel processing have been developed to overcome this limitation.

Keywords: X-ray spectroscopy; EXAFS; XANES; Photoelectron diffraction; Core-level photoemission

1. Introduction

The development of X-ray spectroscopy theory has roughly paralleled that of modern synchrotron radiation X-ray sources over the past three decades. After the introduction of synchrotron facilities, accurate multiple-scattering methods were developed for photoelectron diffraction in the mid-1970s [1,2]. These LEED-like methods were most effective at relatively low kinetic energies (below a few hundred eV), but became rather slow computationally at higher energies. Very significant advances in multiple-scattering (MS) theory have revolutionized the techniques of extended X-ray absorption fine structure (EXAFS) and X-ray photoelectron diffraction (XPD) for local structure determinations [3–5]. Remarkably the advances were of a similar nature, but applied to different spectroscopies by different groups. For example, the development of curved wave single-scattering theories to replace the less

*Corresponding author. Tel.: +1-510-486-6160; fax: +1-510-486-4995.
E-mail address: vanhove@lbl.gov (M.A. Van Hove).

0368-2048/02/$ – see front matter
PII: S0368-2048(02)00204-9

accurate plane wave approximation had originally been applied to EXAFS by Rehr et al. [6] and subsequently to XPD by Fadley et al. [7]. As a second example, the development of the separable approximation for the electron propagator by Rehr and Albers made MS calculations efficient and accurate both for EXAFS [8] and XPD [9]. These parallel developments were possible since the underlying physics of these spectroscopies is similar, involving the photo excitation of an energetic photoelectron and the creation of a deep core hole. As a result of these '2nd generation theory' developments, the basic theory of the fine structure in EXAFS and XPD can be considered as well understood. These developments are discussed in detail in several reviews [3,4].

Significant progress has also been made in 'third generation' theories, in parallel with the current series of high brilliance X-ray sources, such as the ALS and APS. This progress is largely aimed at understanding the physics of the near edge structure, i.e., the structure within about 30 eV of threshold where strong chemical (and hence strong MS contributions) and many-body effects are most important. Such calculations are highly demanding computationally. However, the development of efficient Lanczos iterative MS algorithms, first in XPD [10] and then in XAS [11], gives hope that this regime may eventually be amenable to accurate calculations. Nonetheless, a fully quantitative treatment remains elusive, due to a host of complications, e.g., full potential corrections and many body effects such as core-hole effects and inelastic losses. The development of efficient theory has also given rise to several ab initio codes for XAS calculations in arbitrary systems, for example, CONTINUUM [12], EXCURVE [13], FEFF [14,15] and GNXAS [16]. This development was revolutionary in that it provided accurate theoretical EXAFS standards which eliminated the need for the tabulated phase shifts and greatly simplified the analysis of experiment. Similarly codes for XPD were developed, e.g. MSCD [17,18] and EDAC [10,19].

In the remainder of this article we summarize the key concepts that have led to the current theories, emphasizing the parallel developments in X-ray spectra and photoelectron diffraction.

2. Key developments in theory

Formal theories of XAS and XPD generally start from Fermi's Golden Rule. Thus the X-ray-absorption coefficient μ at X-ray energy $\hbar\omega$ is given by

$$\mu(E) \sim \sum_f |\langle i|\mathbf{A}\cdot\boldsymbol{p}|f\rangle|^2 \delta(E - E_f), \tag{1}$$

where $E = \hbar\omega - E_i$ is the photoelectron energy, $\mathbf{A}\cdot\boldsymbol{p}$ is the coupling to the X-ray field with vector potential $\mathbf{A}$, and the sum is over unoccupied final states. Similarly in core photoemission the photocurrent in a direction $\vec{k}$ is given by:

$$\sigma(\vec{k}) = |\langle i|\mathbf{A}\cdot\boldsymbol{p}|\vec{k}\rangle|^2 \delta(E - E_k), \tag{2}$$

where $|\vec{k}\rangle$ represents a time-reversed scattering state in the direction of the detector. Most practical calculations are based on: (a) the dipole-approximation and (b) the reduction of the Golden Rule to a one-electron approximation. Although the question of which one-electron states to use in a one-electron theory is not unambiguous, much current work is based on the 'final-state rule.' This rule asserts that final states should be calculated in the presence of an appropriately screened core-hole, and all many-body effects and inelastic losses are lumped into a complex valued optical potential. This approximation is used in FEFF and many other codes. Another often used approach for calculating XANES is the atomic multiplet theory [20,21]. A challenge for the future is to improve on these approximations.

2.1. Green's function formalism

An important formal development in modern theories of X-ray spectra is the replacement of explicit calculations of wave functions or scattering states in the Golden Rule with a Green's function approach [22,23]. Calculations of final states is often a computational bottleneck, and can only be carried out efficiently for systems with symmetry, e.g., atoms, small molecules, or crystalline solids. However, many systems of interest lack such symmetry. Also band structure methods which are often used for solids [24,25] generally ignore important effects such as the core-hole and lattice vibrations, which

spoil exact crystal symmetry. Thus instead of explicitly calculating final states, it is often preferable to express the result in terms of the one-electron Green's function or photoelectron propagator in real space, $G(E) = \Sigma_f |f\rangle\langle f|/(E - E_f + i0^+)$, which implicitly sums over all final states. In terms of G, the X-ray absorption coefficient becomes

$$\mu(E) \sim -\frac{1}{\pi} \mathrm{Im}\langle i|\, \hat{\epsilon}\cdot\mathbf{r}'\, G(\mathbf{r}', \mathbf{r}, E)\, \hat{\epsilon}\cdot\mathbf{r}|i\rangle. \quad (3)$$

Within MS theory the propagator $G(\mathbf{r}, \mathbf{r}', E) = \Sigma_{L,L'} R_L(\mathbf{r}) G_{L,L'} R_{L'}(\mathbf{r}')$ can be factored. Then the expression for μ can be reduced to a calculation of atomic dipole-matrix elements $M_L = \langle i|\hat{\epsilon}\cdot\mathbf{r}|L\rangle$ and a propagator matrix $G_{L,L'}$. Moreover, the matrix $G_{L,L'}$ can be re-expressed as a sum over all MS paths that a photoelectron can take away from the absorbing atom and back [22], and thus gives rise to the path expansion which has been used both in EXAFS and XPD [4]. The relativistic generalization [26] is similar; however relativistic effects (e.g, spin–orbit effects) are biggest in the atomic cores and mostly affect the dipole matrix elements. Since $G_{L,L'} = G^c_{L,L'} + G^{sc}_{L,L'}$ naturally separates into intra-atomic contributions from the central atom and from MS, the XAS factorizes as $\mu = \mu_0(1 + \chi)$. Hence the structure in μ depends both on an (embedded) atomic background μ_0 and on the MS or fine structure signal χ. This result is consistent with the experimental definition of XAFS $\chi = (\mu - \mu_0)/\Delta\mu_0$, where $\Delta\mu_0$ is the jump in the smooth atomic-like background. For XANES, however, the MS expansion is often carried to all orders (full MS) by matrix inversion [12,27] and is then equivalent to 'exact' treatments, e.g., the KKR band structure method [23].

In MS theory the scattering potentials v_i are implicitly contained in the scattering t-matrices $t = v + vGt$ at each site, in terms of partial wave phase shifts, $t_l = \exp(i\delta_l)\,\sin(\delta_l)$. The calculations simplify for electrons of moderate energy, since scattering depends largely on the density in the core of an atom, where spherical symmetry is a good approximation. Thus the Coulomb part is well described by an overlapped atomic charge density and the overlapped muffin-tin approximation (i.e., the Mattheiss prescription), while the exchange term can be well approximated by a local self energy (see below). However, these approximations can be inadequate for XANES and valence-level photoelectron diffraction, where chemical effects and charge transfer are important, in which case self-consistent (SCF) calculations are necessary. Muffin-tin corrections can also be important at low electron kinetic energies, and hence the development of a full-potential generalization is desirable [28,29].

Another advantage of the Green's function formalism is that it simplifies the treatment of inelastic losses, i.e. the electron mean free path. Indeed, a crucial difference between ground state electronic structure calculations and excited states is the need in the latter for a complex, energy dependent 'self-energy' $\Sigma(E)$. This mean free path differs from that, say in LEED, since it depends on the core-hole lifetime, and also on various many-body relaxation effects. The self-energy is essentially a dynamically screened exchange interaction, which is the analog of the exchange-correlation potential V_{xc} of density functional theory. The self energy varies by about 10 eV over EXAFS energies, and leads to systematic shifts in energy of XAS peaks from their ground state positions. FEFF and other XAFS codes often use an approximate electron gas Hedin–Lundqvist self-energy. A challenge is to develop improved self-energy approximations.

2.2. Curved-wave multiple scattering theory

One of the most important theoretical developments in XAS and XPD was that of efficient curved-wave scattering theory. Because of curved wave effects, exact MS calculations can be very time-consuming and at high energies can only be carried out for low-order MS paths [30]. For the same reason, band structure approaches are generally limited to energies below a few hundred eV. A major drawback of some early treatments of XAFS and XPD was the use of the crude plane-wave approximation (PWA) to describe scattering of the photoelectron. Subsequently, Rehr et al. showed how single scattering theory could be recast in a form analogous to the PWA but with an effective, curved wave scattering amplitude f_{eff}. This quantity has an expansion in partial waves analogous to the back-

scattering amplitude in the PWA, but has a substantial phase shift at all energies, which explains why the PWA is almost always a poor approximation. In an extension of this approach, an analogous effective scattering amplitude was derived for XPD, and applied by Sagurton et al. [7].

One of the major theoretical advances of 2nd generation theories was the development of efficient approximations to treat MS. Some of the first such approaches were developed by Barton and Shirley [31] for XPD. In an effort to improve on their approach, an efficient scattering matrix formalism was derived, based on a separable representation of the free propagator $G(E)$ [8]. This 'Rehr–Albers' approach turned out to overcome many of the computational difficulties of the MS expansion, i.e., (1) the large angular-momentum basis; (2) the proliferation of MS paths; and (3) the need for correlated MS Debye–Waller factors. The first difficulty was overcome in two steps. First, by using rotation matrices, successive bonds in a path are rotated to the z-axis, thus reducing the problem to a calculation of 'z-axis propagators' [8]. Propagators along the z-axis have greatly simplified mathematical properties; although the terminology 'z-axis propagator' is recent, these quantities have a long history and have been rediscovered several times [32,33]. However it has also been found that it is both stable and accurate to use the recursive calculations of the RA separable representation, as we now discuss. A detailed discussion of the convergence of the RA approach has also been carried out [17]. The second step of the RA method is an exact, separable representation of the z-axis propagators, which was inspired by the low-energy approximation of Barton and Shirley [31]. Together this yields

$$G_{L\mathbf{R},L'\mathbf{R}'} = \frac{e^{ikR''}}{kR''} \Sigma_\lambda Y_{L,\lambda} \tilde{Y}_{\lambda,L'}, \tag{4}$$

where $\mathbf{R}'' = \mathbf{R}' - \mathbf{R}$. The coefficients Y and $\tilde{Y}$ converge rapidly in powers of $1/kR$, and hence the representation can be severely truncated. The approach becomes exact at low energies or for single scattering, and typically only six terms suffice to converge within experimental precision over the full range of wave numbers in EXAFS experiment. The advantage of the separable representation is that it permits one to combine and then sum all the factors involving L at a given site into a scattering matrix $F_{\lambda',\lambda} = \Sigma_L \tilde{Y}_{\lambda',L} t_L Y_{L,\lambda}$; this is the analog of the PWA and yields an accurate curved-wave XAFS formula with the usual scattering amplitudes $f(\theta)$ replaced by low-order (6×6) matrices. With separable propagators, the MS expansion can naturally be calculated as a sum over MS paths. For EXAFS, for example, one obtains

$$\chi(k) = S_0^2 \sum_{\text{paths}} \frac{|f_{\text{eff}}(k)|}{kR^2} \sin(2kR + \Phi_k)\, e^{-2R/\lambda_k} e^{-2\sigma^2 k^2}, \tag{5}$$

where $k = [2(E - E_0)]^{1/2}$ is the wavenumber measured from threshold E_0, λ_k is the XAFS mean-free path, and σ is the rms fluctuation in the effective path length $R = R_{\text{path}}/2$. This expression has the same form as the famous XAFS equation of Sayers, Stern and Lytle [34], However, it must be stressed that all quantities in Eq. (3) must be redefined to include curved-wave and many-body effects. For example, the plane wave back-scattering amplitude is replaced by an effective curved-wave scattering amplitude $f_{\text{eff}}(k)$ (after which the FEFF codes are named), and which was not in the original formula. For XANES, however, exact propagators are needed. It turns out that the RA approach still provides a stable and efficient algorithm [35] which has been implemented in the FEFF codes.

2.3. Accurate Green function expansions

As discussed in the previous sections, the MS series can be summed to all orders by means of various numerical algorithms. The propagator matrix $G_{L,L'}$ is thus calculated exactly, implicitly including all MS paths up to infinite order. In a cluster approach, the electron wave function can be written as a combination of outgoing scattered waves $h_L^{(+)}$ centered at the positions of the cluster atoms $\mathbf{r}_\alpha$ as

$$\phi(\mathbf{r}) = \sum_{\alpha,L} \phi_{\alpha,L} h_L^{(+)}[k(\mathbf{r} - \mathbf{r}_\alpha)], \tag{6}$$

where k is the electron momentum and the expansion coefficients $\phi_{\alpha,L}$ can be shown to satisfy the following self-consistent relation (in matrix notation) [10]:

$$\phi_\alpha = \phi^0_\alpha + t_\alpha \sum_{\beta\neq\alpha} G_{\alpha\beta}\phi_\beta \qquad (7)$$

in terms of the coefficients of the direct wave expansion $\phi^0_{\alpha,L}$ (i.e., in the absence of MS) [10]. Here, t_α is the scattering matrix of atom α and $G_{\alpha\beta}$ is the Green function that propagates the wave function from atom β to atom α.

The separable approximation discussed above yields the computationally expensive products involving $G_{\alpha\beta}$ by expanding this operator as a sum of products of matrices of smaller size, which leads to the concept of electron path. This approximation becomes cumbersome when the number of cluster atoms and scattering paths that contribute in the calculation of the wavefunction is large. In such cases, an alternative approach consists in evaluating Eq. (7) directly, without making any approximation to the propagator. For small clusters, as in the case of emission or absorption in free molecules, Eq. (7) can be solved by direct inversion. This has been done in particular for calculating the photoemission spectra of fixed-in-space diatomic molecules, for which extensive sets of experimental data have been collected [36–38].

Previously, free-molecule studies were limited to orientationally-averaged measurements, thus limiting the information derivable from the data. The dependence of such fixed-in-space angular distributions on photon energy provides an exciting new probe of the molecular electronic structure and dynamics. Particularly important are the energies for which the so-called shape resonances appear in the continuum, since the experimental angular profiles show radical changes. The theoretical calculation of the photoemission spectra in this range of energies requires the inclusion of non-spherical effects in the scattering of the electron off the molecular centers [28]. The comparison between experiment and theory shows excellent agreement, in particular regarding the angular distribution of photoemission near the so-called shape resonance, which is highly sensitive to the details of the potential [29]. As an example, Fig. 1 shows the angular distribution of electrons photoemitted from the 1s-shell of C in the CO molecule, when the incident light is linearly polarized and the polarization vector ε is parallel to the molecular axis. The upper panel shows the angular distribution when the kinetic energy of the electron is

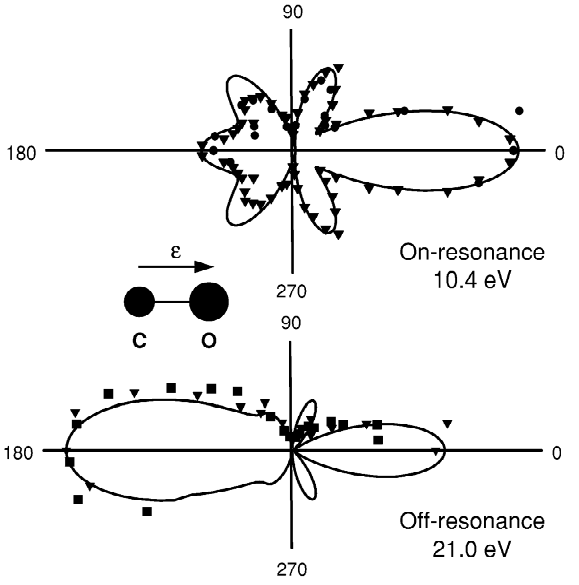

Fig. 1. Theoretical calculation of the angular distribution of electrons photoemitted from the 1s-shell of C in CO. The light polarization ε is parallel to the C–O axis (solid line), with the O atom toward 0° (right side), and the C atom toward 180° (left side). The kinetic energy of the electrons is 10.4 eV in the upper panel and 21.0 eV in the lower panel. The black squares, circles and triangles are experimental data from Refs. [39–41]. The intensity is plotted in arbitrary units.

at the shape resonance ($E = 10.4$ eV), and the lower panel shows the angular distribution when the kinetic energy is well above it ($E = 21.0$ eV). The theoretical calculations agree well with recent experimental data [39–41]. For kinetic energies above the shape resonance, the electron intensity along the C direction is higher than the electron intensity along the O direction [37]. This behavior is reversed at the shape resonance. The shape resonance thus implies special conditions of scattering for which the directly emitted wave and the scattered waves combine to create constructive interference along the O direction.

For much larger clusters of atoms, direct inversion of Eq. (7) is computationally prohibitive, and one has to rely on iterative techniques that yield the wave function coefficients by successive refinement. One such method is the recursion method, which is implemented in the fully automated code EDAC (Electron Diffraction in Atomic Clusters) [10,19]. This program can calculate photoelectron angle and energy distributions without any external parameters.

In particular, scattering phase shifts and muffin-tin potentials are automatically obtained inside the code.

The recursion method has the advantage of avoiding divergences in the MS series that would otherwise lead to limited numerical accuracy. This method can also be applied to systems where clusters composed of thousands of atoms are needed. As an example of this, Fig. 2 illustrates the convergence of the emission intensity from a subsurface Cu atom as a function of the number of atoms used to simulate a surface. An *R*-factor analysis has been used to quantify the degree of convergence of the emission intensity as compared to the case of $N = 1856$ atoms. The latter case is taken as a reference converged calculation. The inset shows the actual intensity as a function of the azimuthal angle of emission, showing that even for 900 atoms there are sizable differences between the angular scan curves.

Several other approaches have been developed for speeding up such calculations. Promising methods include a convergent N^2-scaling iterative method [42], the continued-fraction recursion method [43,10] repartitioning [44] and iterative approaches which can provide substantial improvements on the conventional LU decomposition. In particular modern Lanczos algorithms such as the Lanczos/LU have proved to be both stable and accurate [11]. Even more dramatic reductions can be obtained from parallel MS algorithms. These scale as $A + B/N$, where N is the number of processors, and hence can increase the speed by orders of magnitude [11,18]. For example, parallelization has been implemented in the FEFF8 XAS code with the MPI (message-passing-interface) protocol [45]. As a result of these advances, an improvement in computational speed of about two orders of magnitude has been achieved, making such calculations practicable in complex systems of order 1000 atoms.

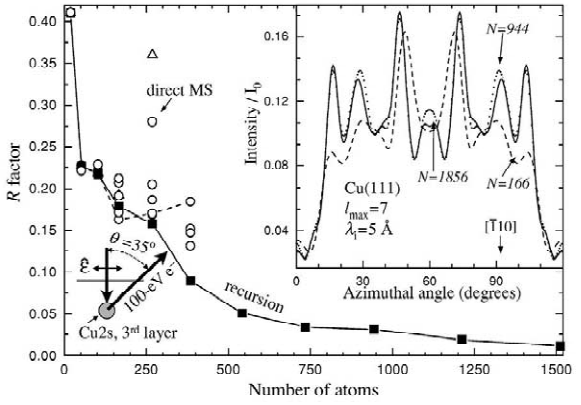

Fig. 2. *R*-factor (Eq. (34) of Ref. [10]) variation with the number of atoms N for Cu 2s photoemission from the third layer of a Cu(111) surface. Azimuthal scans have been considered with a polar angle of emission of 35°, a photoelectron energy of 100 eV, and p-polarized light under normal incidence conditions, as shown schematically in the lower left corner of the figure. The inset shows the intensity as a function of the azimuthal angle for various cluster sizes, as indicated by labels. The intensity is normalized to that of the direct emission without inelastic attenuation I_0.

2.4. Quantitative calculations and applications

Fully quantitative calculations require several other considerations, in particular the effects of thermal disorder and inelastic losses. The effects of disorder are also of crucial importance both in XAFS and XPD, as they lead to damping of the rapidly oscillating fine structure amplitudes. A useful simplification is the cumulant expansion which gives an efficient parameterization of such disorder [46,47] in terms of a few moments or cumulants of the vibrational distribution function. One of the problems with the one-electron approximation is an overestimation of fine structure amplitudes, which is corrected phenomenologically by an amplitude reduction factor S_0^2. This factor is typically between 0.7 and 0.9 and arises largely from intrinsic losses in the creation of the core hole, i.e., the multi-electron shake-up and shake-off excitations [48]. Partly due to the difficulty of calculating S_0^2, the determination of coordination numbers from EXAFS is typically accurate only to ± 1. Recently, however, a quasi-boson formalism has been introduced for such calculations which treats both extrinsic and intrinsic losses, as well as interference between them [49]. The interference terms tend to suppress excitations near threshold, which may explain why the existence of sharply defined multi-electron peaks in XANES has been controversial [50]. Preliminary numerical results for S_0^2 from this approach are quite promising. Similar theoretical developments have been carried out for core photoemission spectroscopy (PES). For example, Ref. [51] discusses the transition from the adiabatic to the sudden limit in PES.

Because the underlying physics is similar, the same approaches can be applied to many other spectroscopies, e.g., electron energy loss spectra (EELS) [52], circular dichroism (XMCD) [53], etc., in addition to XPS. For example, FEFF has also been adapted for studies of diffraction anomalous fine structure (DAFS) [54] and the X-ray elastic scattering amplitude [55].

3. Combined view of initial and final states in photoemission

According to the Golden Rule, the photocurrent in the one-step model is effectively determined by the matrix element between the initial and the final states. To illustrate the various contributions to the matrix element it is convenient to represent both wave functions in position space via a direct solution of the Schrödinger equation, instead of the MS procedure. The initial state arises as a stationary solution of the Schrödinger equation for the half space occupied by the solid and its surface with adjacent vacuum. The boundary condition forces the wave function to decay to zero in the vacuum region. The final state arises as a solution defined by outgoing asymptotics which denotes a Cauchy problem rather than a customary boundary value problem for an elliptic type partial differential equation. Instabilities arise which are known to spoil the usual matching algorithms. However, procedures have been developed to convert the asymptotic conditions into an ordinary mixed boundary value problem [56–60].

Thus, the matrix element for such a transition can be roughly described as an integral over two factors, each varying monotonically with one of the two charge densities. If one neglects the phases, regions with large initial and final state charge distributions should contribute relatively more. A strong local variation of the final state is observed from the calculations, in strength similar to what is common for the initial states, see Fig. 3. The consideration of both contributions can lead to a characterization of emissions as arising from specific orbitals and sites of the initial state. The dipole operator in the matrix

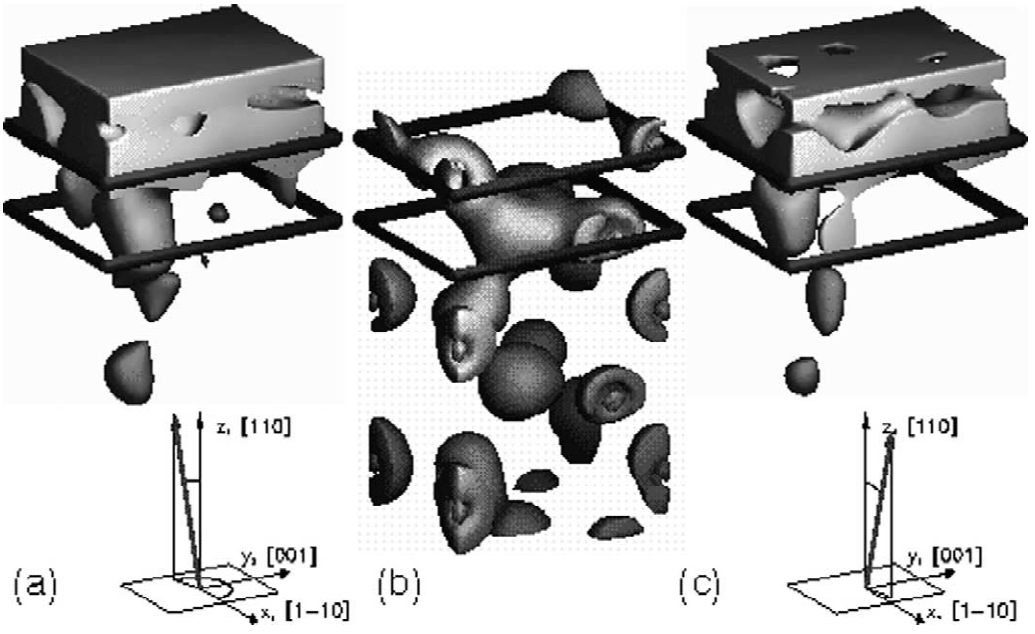

Fig. 3. Constant-square modulus plots of final (a and c) and initial (b) states for the GaAs(110) surface. The final states differ in the azimuthal escape angle: (a) $\phi = 195°$, and (c) $\phi = 15°$. The surface is indicated by the rectangular frames, with surface As atoms at the corners of the upper frame, the solid below and the vacuum above. Coordinate axes are shown at the bottom.

element either in the position or momentum representation contributes primarily through the polarization of the incident light in the long wave case, say of the vacuum ultraviolet light. It thus emphasizes emission into directions parallel to the electric field vector. This is obvious from the momentum representation where the momentum operator takes on the value of the wave vector of that outgoing electron wave carrying the main current. Its product with the vector potential, i.e. the electric field, becomes largest if both are parallel. Similarly, in the position representation the dipole components perpendicular to the main propagation direction of the final state electron cancel by sign reversal within the integration, leaving only the parallel component. Of course, this crude picture does not account for all properties of the shape of the initial state, but it is a good first guide when inspecting the azimuthal patterns [61]. Secondary influences from this operator and others may change the picture, as does for instance the inclusion of the phases of the waves through their interference terms.

In Fig. 3 the charge densities of two outgoing states in near normal emission, $\vartheta = 19.4°$, with opposite azimuths are plotted together with the initial state which does not discriminate between the two directions. The (001) mirror plane of the GaAs(110) surface, which includes the vectors [110] and [1-10] marked at the bottom of this figure, makes both $\mathbf{k}_{\parallel}$ directions equivalent for the initial but not for the final charge density. The latter does not possess the Bloch state property where symmetry related directions can be mapped onto each other by operating solely on the Bloch vector being not visible in the square modulus. Symmetry is broken more severely in the final state through the boundary conditions fixed by the position of the detector because more than one plane wave contributes. Of course, both final states are mirror images of each other. The energies are 4.0 eV below and 17 eV above the valence band maximum for the initial and final state, respectively. The product of initial and final state charge density gives an idea of what can be expected from a photoemission calculation in this case.

The discussion of this section shows that the direct solution of the Schrödinger equation is not only a tool for the calculation of the photocurrent but also yields useful physical pictures of the photoemission mechanism. As a numerical method it shows its strength for angle resolved valence spectroscopy in the VUV light regime. Though not discussed here, it can be understood that procedures residing in band-structure calculations are suitable for the investigation of valence bands via low lying conduction bands.

Acknowledgements

We wish to thank C.S. Fadley for many contributions which helped shape the developments discussed here. We also gratefully acknowledge the contributions to this work from our co-workers, students, and collaborators, especially R.C. Albers, K. Baberschke, G. Brown, L. Campbell, A. Chassé, Y. Chen, C.L. Cocke, R. Dörner, F. Farges, T. Fujikawa, G. George, L. Hedin, B. Hedman, K. Hodgson, A.P. Kaduwela, L. Kipp, A.L. Landers, J. Mustre de Leon, C. R. Natoli, M. Newville, M.H. Prior, B. Ravel, D. Rolles, D. Sayers, E. Shirley, M. Skibowski, C. Solterbeck, E. A. Stern and J. W. Wilkins. This work was supported by the U.S. Department of Energy grant DE-FG06-97ER45623/A000 (JJR), by the Director, Office of Science, Office of Basic Energy Sciences, Division of Materials Sciences and Engineering, of the U.S. Department of Energy under Contract No. DE-AC03-76SF00098, by the Bundesministerium für Bildung, Wissenschaft, Forschung und Technologie (BBWFT) under contract Nos. 05 5FKTAB 1 and 05 605FKA 1, by the Basque Departamento de Educación, Universidades e Investigación, the University of the Basque Country UPV/EHU (9/UPV 00206.215-13639/2001), and the Spanish Ministerio de Ciencia y Tecnología (MAT2001-0946). RDM acknowledges financial support by the Gipuzkoako Foru Aldundia (Gipuzkoa Fellows Program).

References

[1] J.B. Pendry, Surf. Sci. 57 (1976) 679.
[2] S.Y. Tong, M.A. Van Hove, Sol. St. Comm. 19 (1976) 543.
[3] J.J. Rehr, R.C. Albers, Rev. Mod. Phys. 72 (2000) 721.
[4] C.S. Fadley, M.A. Van Hove, Z. Hussain, A.P. Kaduwela, R.E. Couch, Y.J. Kim, P.M. Len, J. Palomares, S. Ryce, S.

Ruebush, E.D. Tober, Z. Wang, R.X. Ynzunza, H. Daimon, H. Galloway, M.B. Salmeron, W. Schattke, Surf. Rev. Lett. 4 (1997) 421.
[5] C.S. Fadley, Y. Chen, R.E. Couch, H. Daimon, R. Denecke, J.D. Denlinger, H. Galloway, Z. Hussain, A.P. Kaduwela, Y.J. Kim, P.M. Len, J. Liesegang, J. Menchero, J. Morais, J. Palomares, S.D. Ruebush, E. Rotenberg, M.B. Salmeron, R. Scalettar, W. Schattke, R. Singh, S. Thevuthasan, E.D. Tober, M.A. Van Hove, Z. Wang, R.X. Ynzunza, Progr. Surf. Sci. 54 (1997) 341.
[6] J.J. Rehr, R.C. Albers, C.R. Natoli, E.A. Stern, Phys. Rev. B 34 (1986) 4350.
[7] M. Sagurton, E.L. Bullock, R. Saiki, A. Kaduwela, C.R. Brundle, C.S. Fadley, J.J. Rehr, Phys. Rev. B 33 (1986) 2207.
[8] J.J. Rehr, R.C. Albers, Phys. Rev. B 41 (1990) 8139.
[9] A.P. Kaduwela, D.J. Friedman, C.S. Fadley, J. Electron Spectros. Relat. Phenom. 57 (1991) 223.
[10] F.J. García de Abajo, M.A. Van Hove, C.S. Fadley, Phys. Rev. B 63 (2001) 075404.
[11] A.L. Ankudinov, C. Bouldin, J.J. Rehr, J. Sims, H. Hung, Phys. Rev. B 65 (2001) 104107.
[12] C.R. Natoli, D.K. Misemer, S. Doniach, F.W. Kutzler, Phys. Rev. A 22 (1980) 1104.
[13] N. Binsted, J.W. Campbell, S.J. Gurman, P.C. Stephenson, SERC Daresbury Laboratory EXCURVE program (unpublished), 1991.
[14] J.J. Rehr, J. Mustre de Leon, S.I. Zabinsky, R.C. Albers, J. Am. Chem. Soc. 113 (1991) 5136.
[15] A.L. Ankudinov, B. Ravel, J.J. Rehr, S. Conradson, Phys. Rev. B 58 (1998) 7565, see also the FEFF URL http://leonardo.phys.washington.edu/feff/.
[16] A. Filipponi, A. Di Cicco, Phys. Rev. B 52 (1995) 15122.
[17] Y. Chen, F.J. García de Abajo, A. Chassé, R.X. Ynzunza, A.P. Kaduwela, M.A. Van Hove, C.S. Fadley, Phys. Rev. B 58 (1998) 13121.
[18] See the MSCD URL http://electron.lbl.gov/mscdpack/mscdpack.html.
[19] See the EDAC URL http://electron.lbl.gov/~edac.
[20] F.M.F. de Groot, J. Electron Spectros. Relat. Phenom. 67 (1994) 529.
[21] A. Kotani, J. Phys. IV France 7 (Colloque C2) (1997) C1–C8.
[22] P.A. Lee, J.B. Pendry, Phys. Rev. B 11 (1975) 2795.
[23] W.L. Schaich, Phys. Rev. B 8 (1973) 4028.
[24] P. Blaha, K. Schwarz, J. Luitz, WIEN98, 1998;
P. Blaha, K. Schwarz, P. Sorantin, S.B. Trickey, Comput. Phys. Commun. 59 (1990) 399.
[25] J.E. Müller, O. Jepsen, J.W. Wilkins, Solid State Comm. 42 (1982) 365.
[26] H. Ebert, Rep. Prog. Phys. 59 (1996) 1665.
[27] P.J. Durham, J.B. Pendry, C.H. Hodges, Comp. Phys. Commun. 25 (1982) 193.
[28] R. Díez Muiño, D. Rolles, F.J. García de Abajo, F. Starrost, W. Schattke, C.S. Fadley, M.A. Van Hove, J. Electron Spectros. Relat. Phenomena 114–116 (2001) 99.
[29] R. Díez Muiño, D. Rolles, F.J. García de Abajo, C.S. Fadley, M.A. Van Hove, J. Phys. B: At. Mol. Opt. Phys. 35 (2002) L359.
[30] S.J. Gurman, N. Binsted, I. Ross, J. Phys. C 19 (1986) 1845.
[31] J.J. Barton, D.A. Shirley, Phys Rev. B 32 (1985) 1906.
[32] R. Nozawa, J. Math. Phys. 7 (1966) 1841.
[33] V. Fritzsche, J. Electron Spectros. Relat. Phenomena 58 (1992) 299.
[34] D.E. Sayers, E.A. Stern, F.W. Lytle, Phys. Rev. Lett. 27 (1971) 1204.
[35] F. Manar, Ch. Brouder, Physica B 208 & 209 (1995) 79.
[36] E. Shigemasa, J. Adachi, M. Oura, A. Yagishita, Phys. Rev. Lett. 74 (1995) 359.
[37] F. Heiser, O. Gessner, J. Viefhaus, K. Wieliczek, R. Hentges, U. Becker, Phys. Rev. Lett. 79 (1997) 2435.
[38] A. Landers, Th. Weber, I. Ali, A. Cassimi, M. Hattass, O. Jagutzki, A. Nauert, T. Osipov, A. Staudte, M.H. Prior, H. Schmidt-Böcking, C.L. Cocke, R. Dörner, Phys. Rev. Lett. 87 (2001) 013002.
[39] E. Shigemasa, J. Adachi, K. Soejima, N. Watanabe, A. Yagishita, N.A. Cherepkov, Phys. Rev. Lett. 80 (1998) 1622.
[40] S. Motoki, J. Adachi, Y. Hikosaka, K. Ito, M. Sano, K. Soejima, A. Yagishita, G. Raseev, N.A. Cherepkpo, J. Phys. B: At. Mol. Opt. Phys. 33 (2000) 4193.
[41] Th. Weber, O. Jagutski, M. Hattass, A. Staudte, A. Nauert, L. Schmidt, M.H. Prior, A.L. Landers, A. Bräuning-Dernian, H. Bräuning, C.L. Cocke, T. Osipov, I. Ali, R. Díez Muiño, D. Rolles, F.J. García de Abajo, C.S. Fadley, M.A. Van Hove, A. Cassimi, H. Schmidt-Böcking, R. Dörner, J. Phys. B: At. Mol. Opt. Phys. 34 (2001) 3669.
[42] H. Wu, S.Y. Tong, Phys. Rev. B 59 (1999) 1657.
[43] A. Filipponi, J. Phys.: Condens Matter 3 (1991) 6489.
[44] T. Fujikawa, J. Phys. Soc. Japan (1993).
[45] W. Gropp, E. Lusk, A. Skjellum, Using MPI: Portable Parallel Programming With The Message-Passing Interface, MIT Press, Cambridge, Mass, 1994.
[46] E.D. Crozier, J.J. Rehr, R. Ingalls, in: D.C. Koningsberger, R. Prins (Eds.), X-Ray Absorption: Principles, Applications, Techniques of EXAFS, SEXAFS, and XANES, Wiley, New York, 1988, p. 375.
[47] G. Dalba, P. Fornasini, J. Synchrotron Rad. 4 (1997) 243.
[48] J.J. Rehr, E.A. Stern, R.L. Martin, E.R. Davidson, Phys. Rev. B 17 (1978) 560.
[49] L. Campbell, L. Hedin, J.J. Rehr, W. Bardyszewski, Phys. Rev. B 65 (2002) 064107.
[50] A. Filipponi, A. Di Cicco, Phys. Rev. B 53 (1996) 9466.
[51] L. Hardin, J. Michiels, J. Inglesfield, Phys. Rev. B 58 (1998) 15565.
[52] T. Sikora, G. Hug, M. Jaouen, J.J. Rehr, Phys. Rev. B 62 (2000) 1723.
[53] A.L. Ankudinov, J.J. Rehr, Phys. Rev. B 56 (1997) R1712; A.L. Ankudinov, J.J. Rehr, Phys. Rev. B 52 (1995) 10214.
[54] J.O. Cross, M.I. Bell, M. Newville, J.J. Rehr, L.B. Sorensen, C.E. Bouldin, G. Watson, T. Gouder, G.H. Lander, Phys. Rev. B 58 (1998) 11215.
[55] A.L. Ankudinov, J.J. Rehr, Phys. Rev. B 62 (2000) 2437.
[56] C.S. Lent, D.J. Kirkner, J. Appl. Phys. 67 (1990) 6353.
[57] Y. Joly, Phys. Rev. Lett. 68 (1992) 950;

Y. Joly, Phys. Rev. B 53 (1996) 13029.
[58] S. Lorenz, C. Solterbeck, W. Schattke, J. Burmeister, W. Hackbusch, Phys. Rev. B 55 (1997) 13432.
[59] C. Solterbeck, O. Tiedje, W. Schattke, J. Electron Spectros. Relat. Phenom. 88–91 (1998) 563.
[60] W. Schattke, Prog. Surf. Sci. 64 (2000) 89.
[61] C. Solterbeck, W. Schattke, J.W. Zahlmann-Nowitzki, K.U. Gawlik, L. Kipp, M. Skibowski, C.S. Fadley, M.A. Van Hove, Phys. Rev. Lett. 79 (1997) 4681.